Cellular Oncology
https://doi.org/10.1007/s13402-019-00471-x

ORIGINAL ARTICLE

Piperlongumine potentiates the antitumor efficacy of oxaliplatin through ROS induction in gastric cancer cells

Peichen Zhang[1] · Lingyan Shi[2] · Tingting Zhang[3] · Lin Hong[3] · Wei He[3] · Peihai Cao[3] · Xin Shen[3] · Peisen Zheng[3] · Yiqun Xia[2] · Peng Zou[3]

Accepted: 13 August 2019

Abstract

Purpose Oxaliplatin is one of the most commonly used chemotherapeutic agents in the treatment of various cancers, including gastric cancer. It has, however, a narrow therapeutic index due to its toxicity and the occurrence of drug resistance. Therefore, there is a pressing need to develop novel therapies to potentiate the efficacy and reduce the toxicity of oxaliplatin. Piperlongumine (PL), an alkaloid isolated from *Piper longum L.*, has recently been identified as a potent agent against cancer cells in vitro and in vivo. In the present study, we investigated whether PL can potentiate the antitumor effect of oxaliplatin in gastric cancer cells.

Methods Cellular apoptosis and ROS levels were analyzed by flow cytometry. Thioredoxin reductase 1 (TrxR1) activity in gastric cancer cells or tumor tissues was determined using an endpoint insulin reduction assay. Western blotting was used to analyze the expression levels of the indicated proteins. Nude mice xenograft models were used to test the effects of PL and oxaliplatin combinations on gastric cancer cell growth in vivo.

Results We found that PL significantly enhanced oxaliplatin-induced growth inhibition in both gastric and colon cancer cells. Moreover, we found that PL potentiated the antitumor effect of oxaliplatin by inhibiting TrxR1 activity. PL combined with oxaliplatin markedly suppressed the activity of TrxR1, resulting in the accumulation of ROS and, thereby, DNA damage induction and p38 and JNK signaling pathway activation. Pretreatment with antioxidant N-acetyl-L-cysteine (NAC) significantly abrogated the combined treatment-induced ROS generation, DNA damage and apoptosis. Importantly, we found that activation of the p38 and JNK signaling pathways prompted by PL and oxaliplatin was also reversed by NAC pretreatment. In vivo, we found that PL combined with oxaliplatin significantly suppressed tumor growth in a gastric cancer xenograft model, and effectively reduced the activity of TrxR1 in tumor tissues. Remarkably, we found that PL attenuated body weight loss evoked by oxaliplatin treatment.

Peichen Zhang, Lingyan Shi, Tingting Zhang and Lin Hong contributed equally to this work.

Electronic supplementary material The online version of this article (https://doi.org/10.1007/s13402-019-00471-x) contains supplementary material, which is available to authorized users.

✉ Yiqun Xia
Yiqunxia@yeah.net

✉ Peng Zou
zoupeng@wmu.edu.cn

Peichen Zhang
zpc52520@163.com

Lingyan Shi
sly52520@163.com

Tingting Zhang
920236374@qq.com

Lin Hong
1120753338@qq.com

Wei He
1015307398@qq.com

Peihai Cao
465826652@qq.com

Xin Shen
1114239370@qq.com

Peisen Zheng
980406643@qq.com

Extended author information available on the last page of the article

Published online: 06 September 2019

Conclusions Our data support a synergistic effect of PL and oxaliplatin and suggest that application of its combination may be more effective for the treatment of gastric cancer than oxaliplatin alone.

Keywords Gastric cancer · Thioredoxin reductase 1 · Reactive oxygen species · Piperlongumine · Oxaliplatin

Abbreviations

PL	Piperlongumine
ROS	Reactive oxygen species
TrxR1	Thioredoxin reductase 1
NAC	N-acetyl-L-cysteine
JNK	c-Jun N-terminal kinase
p38	p38 mitogen-activated protein kinase.

1 Introduction

Oxaliplatin is a potent chemotherapeutic agent that is widely used for the treatment of various cancers including gastric cancer [1, 2]. Gastric cancer is one of the most commonly diagnosed malignancies and remains an important cause of mortality worldwide. Although surgical resection may be curative in early stages of the disease, chemotherapy still remains the cornerstone for the treatment of patients diagnosed with advanced stages [3, 4]. However, the clinical application of oxaliplatin is limited due to drug resistance and side effects [5, 6]. Therefore, it is of great significance to develop new agents to improve the efficacy and reduce the toxicity of oxaliplatin.

Thioredoxin reductase 1 (TrxR1) is a selenocysteine containing flavoenzyme that plays a critical role in regulating intracellular redox balances [7]. TrxR1 has been found to be up-regulated in a variety of human tumors and to be associated with increased tumor growth, drug resistance and a poor patient outcome [8, 9]. Moreover, it has been found that TrxR1 inactivation by chemical inhibitors may reverse tumor growth and sensitize cancer cells to chemotherapeutic drugs, suggesting that TrxR1 may serve as an attractive therapeutic target for anticancer drug development [10–13]. Based on this notion, the development of novel inhibitors of TrxR1 as potential antitumor agents has gained attention during recent years [14–16].

Piperlongumine (PL), a natural product isolated from *Piper longum L.*, has recently been identified as a potent cytotoxic agent against cancer cells in vitro and in vivo [17, 18]. It has been found that PL treatment may increase ROS levels in cancer cells, which in turn underlie the cancer cell killing activity of PL [19, 20]. Recent studies have additionally shown that PL can increase the sensitivity of cancer cells to radiation and chemotherapy [21–23]. In the present study, we investigated whether PL can enhance the antitumor efficacy of oxaliplatin in gastric cancer cells. We found that PL significantly enhanced oxaliplatin-induced growth inhibition of these cells and that TrxR1 activity is involved in their synergistic effect both in vitro and in vivo. Our data suggest that PL and oxaliplatin combination treatment of gastric cancer may be more effective than oxaliplatin alone.

2 Materials and methods

2.1 Cell culture and reagents

Piperlongumine, oxaliplatin, BMS-582949 and SP600125 were purchased from Selleck Chemicals (Houston, TX, USA). N-acetyl-L-cysteine (NAC) was purchased from Sigma (St. Louis, MO, USA). SGC-7901, BGC-823, AGS and HCT116 cells were obtained from the Institute of Biochemistry and Cell Biology, Chinese Academy of Sciences. The cells were routinely grown in RPMI-1640 medium or McCoy's 5A medium containing 10% fetal bovine serum in an incubator with a humidified atmosphere of 5% CO_2 at 37 °C. SGC-7901-TrxR1 and SGC-7901-Vehicle cells were generated and characterized in a previous study [24]. The cells were cultured in RPMI-1640 medium containing 10% fetal bovine serum at 37 °C, and maintained by the addition of G418. Antibodies including anti-TrxR1 and anti-GAPDH were purchased from Santa Cruz Biotechnology (Santa Cruz, CA, USA). Antibodies including anti-p-p38, anti-p38, anti-p-JNK, anti-JNK, anti-mouse IgG-HRP and anti-rabbit IgG-HRP were purchased from Cell Signaling Technology (Danvers, MA, USA). The anti-γ-H2A.X antibody was purchased from Abcam (Cambridge, MA, USA), whereas the anti-53BP1 antibody was purchased from Novus Biologicals (Littleton, CO, USA). A FITC Annexin V apoptosis Detection Kit I and Propidium Iodide (PI) were purchased from BD Pharmingen (Franklin Lakes, NJ, USA).

2.2 Cell viability assay

Cells were seeded in 96-well culture plates at a density of 8×10^3 cells per well and allowed to attach overnight in complete growth medium. Next, the cells were treated with PL or oxaliplatin alone or their combination at the indicated doses. At 24 h after treatment, cell viability was

determined using a methyl thiazolyl tetrazolium (MTT) assay. The combination index (CI) of drug interaction was determined using the Chou-Talalay method [25]: CI = 1, additive interaction; CI > 1, antagonistic interaction; CI < 1, synergistic interaction.

2.3 Cell apoptosis assay

Cells were grown in 6-well culture plates and treated with PL, oxaliplatin, or the combination for 24 h. Next, floating and adherent cells were harvested and washed twice with

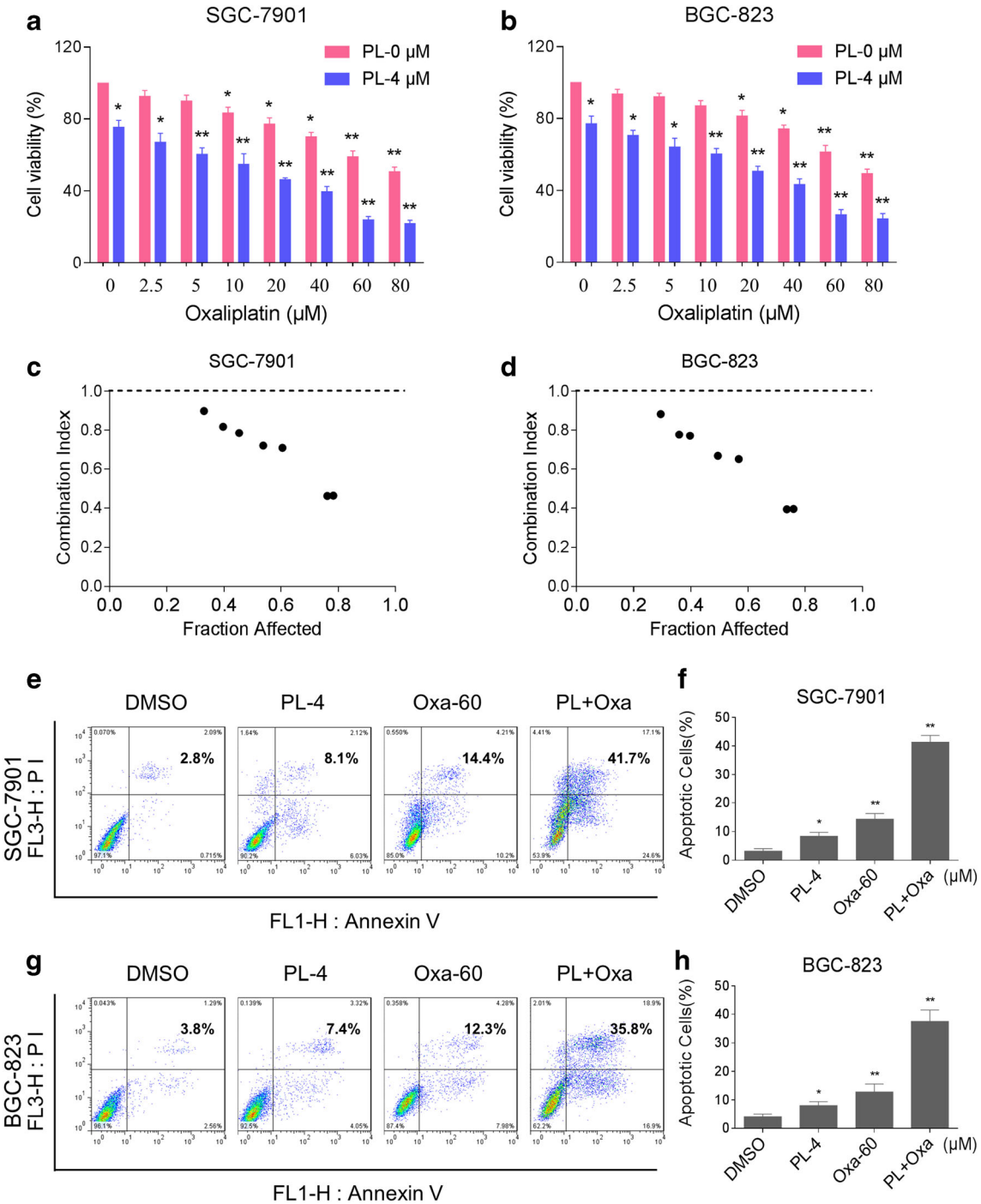

Fig. 1 PL synergistically increases the cytotoxicity of oxaliplatin in gastric cancer cells. a-b SGC-7901 and BGC-823 cells were treated with PL or oxaliplatin alone or their combination at the indicated doses. At 24 h after treatment, cell viability was determined by MTT assay. (**c**-**d**) Combination index (CI) values of PL combined with oxaliplatin were calculated using Calcusyn software. **e-h** SGC-7901 and BGC-823 cells were treated with PL (4 μM) or oxaliplatin (60 μM) alone or their combination (4 μM PL and 60 μM oxaliplatin). At 24 h after treatment, apoptosis was determined by Annexin-V/PI staining and flow cytometry, after which the percentage of apoptotic cells in the treatment groups was calculated. Data represent similar results from three independent experiments (* $p < 0.05$, ** $p < 0.01$)

ice-cold PBS. The washed cell samples were resuspended in 500 μl binding buffer containing 3 μl Annexin-V for 10 min and 2 μl PI for 15 min in the dark and, subsequently, evaluated for apoptosis using a FACSCalibur flow cytometer.

2.4 Reactive oxygen species measurement

Cells were grown in 6-well culture plates and treated with PL, oxaliplatin, or the combination for 2 h. Next, the cells were stained with 10 μM DCFH-DA (Beyotime Biotech, Nantong, China) for 30 min in the dark and collected after which fluorescence intensity was analyzed using a FACSCalibur flow cytometer. In some experiments, cells were pretreated with 5 mM NAC for 2 h prior to compound exposure.

2.5 Western blot analysis

Cells were grown in 6-well culture plates and treated with PL, oxaliplatin, or the combination for the indicated time periods. Next, the cells were lysed with lysis buffer and protein concentrations were determined using the Bradford assay (Bio-Rad, Hercules, CA). The same amounts of proteins were separated by electrophoresis on SDS-polyacrylamide gels and electroblotted onto polyvinylidene difluoride membranes. Five percent non-fat milk was used to block nonspecific binding for 1.5 h at room temperature. Protein bands were probed using specific primary antibodies, detected using horseradish peroxidase conjugated secondary antibodies, and visualized using an ECL kit (Bio-Rad, Hercules, CA). ImageJ software was used to analyze immunoreactive protein bands.

2.6 TrxR1 activity measurement in cells or tumor tissues

Cells were grown in 6-well culture plates and treated with PL, oxaliplatin, or the combination for the indicated times. Next, the cells were lysed with lysis buffer and protein concentrations were determined using the Bradford assay. TrxR1 activity in cell lysates or tumor tissues was determined using an endpoint insulin reduction assay as previously described [24]. Briefly, cell extracts containing 100 μg total protein were incubated in a final reaction volume of 50 μl containing 0.3 mM insulin, 100 mM Tris-HCl (pH 7.6), 3 mM EDTA, 660 μM NADPH, and 15 μM *E. coli* Trx (Sigma, St. Louis, MO) for 30 min. The reactions were terminated by adding 200 μl 1 mM DTNB in 6 M guanidine hydrochloride (pH 8.0). A blank control sample (containing everything except Trx) was treated in the same manner. The absorbance was measured using a SpectraMax iD3 microplate reader (Molecular Devices, USA) at 412 nm, and the activity was expressed as percentage of the blank control.

Fig. 2 PL and oxaliplatin cooperate to trigger ROS-dependent apoptosis in gastric cancer cells. a SGC-7901 and BGC-823 cells were treated with PL (4 μM) and oxaliplatin (60 μM) combination for the indicated time periods, after which intracellular ROS levels were determined by flow cytometry. **b** SGC-7901 and BGC-823 cells were treated with PL (4 μM) or oxaliplatin (60 μM) alone or their combination (4 μM PL and 60 μM oxaliplatin). At 2 h after treatment, intracellular ROS levels were measured by flow cytometry. **c** SGC-7901 and BGC-823 cells were pretreated with 5 mM NAC for 2 h before combined treatment (4 μM PL and 60 μM oxaliplatin). At 2 h after treatment, intracellular ROS levels were measured by flow cytometry. **d** SGC-7901 and BGC-823 cells were pretreated with 5 mM NAC for 2 h before exposure to PL (4 μM) and oxaliplatin (60 μM) combination. At 24 h after treatment, cell viability was determined by MTT assay. **e**-**h** SGC-7901 and BGC-823 cells were pretreated with 5 mM NAC for 2 h before exposure to PL (4 μM) and oxaliplatin (60 μM) combination for 24 h. Apoptosis was determined by flow cytometry, after which the percentage of apoptotic cells in the treatment groups was calculated. Data represent similar results from three independent experiments (* $p < 0.05$, ** $p < 0.01$)

2.7 Immunofluorescence

Cells were grown on coverslips and treated with PL, oxaliplatin, or the combination for 20 h. Next, the cells were fixed in 4% paraformaldehyde for 15 min, followed by incubation in a permeabilization solution for 30 min at room temperature. The coverslips were subsequently washed with PBS three times and incubated with blocking solution for 1 h at room temperature. Next, a primary antibody (53BP1, 1:2000 dilution) in blocking solution was added and the cells were incubated overnight at 4 °C, washed with blocking solution, and incubated with blocking solution containing a DyLight 488 conjugated secondary antibody for 1.5 h at room temperature. Finally, the coverslips were washed, mounted with DAPI stain and analyzed using a Leica fluorescence microscope.

2.8 In vivo antitumor assay

Five-week-old, athymic BALB/c nu/nu female mice (total n = 44) were used for in vivo experiments. All animals were handled according to the Institutional Animal Care and Use Committee (IACUC) guidelines, Wenzhou Medical University. SGC-7901 cells (5×10^6 cells in 100 μl PBS) were harvested and injected subcutaneously into the right flanks of the mice. Next, the mice were divided into four experimental groups on randomization and blinding, with seven mice in each group. Similarly, HCT116 cells (5×10^6 cells in 100 μl PBS) were harvested and injected subcutaneously into the right flanks of the mice. Next, the mice were divided into four experimental groups on randomization and blinding, with four mice in each group. The mice were treated with PL, oxaliplatin, or the combination by intraperitoneal (i.p.) injection once every other day at the indicated doses. At the end of the experiment, the mice were sacrificed and tumors were

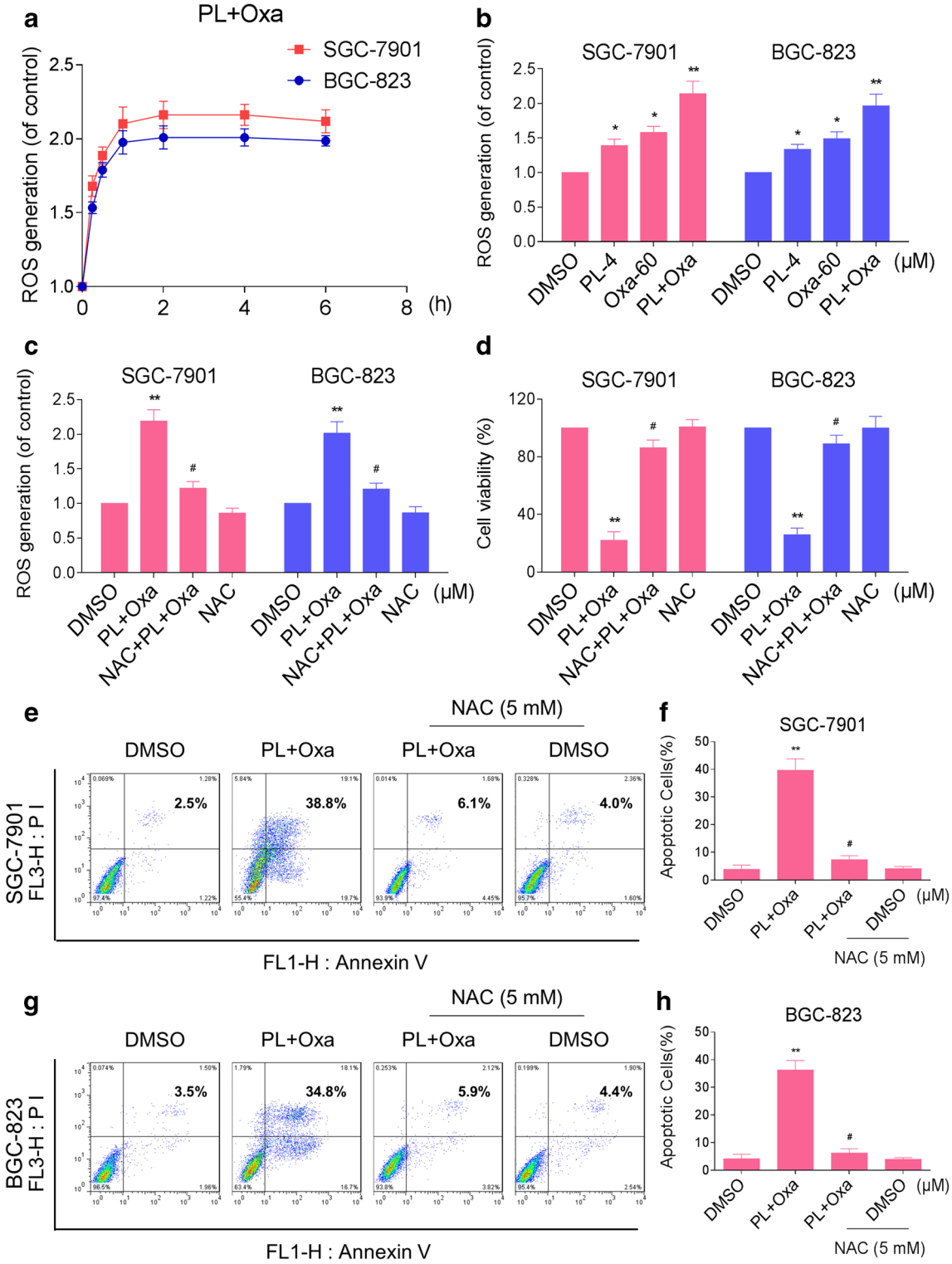

harvested and weighed. Different samples were prepared for histology and protein expression analyses. Tumor sizes were determined by measuring length (l) and width (w) to calculate their volumes ($V = 0.5 \times l \times w^2$).

2.9 MDA assay

For this assay, the harvested tumor tissues were homogenized and sonicated in RIPA buffer on ice. The protein

concentrations were determined using the Bradford assay (Bio-Rad, Hercules, CA). The tumor tissue proteins were normalized according to their concentrations and subjected to a MDA assay according to the instructions provided by the Lipid Peroxidation MDA assay kit (Beyotime Institute of Biotechnology, Nantong, China). The MDA levels were determined using a multimode microplate reader (SpectraMax M5, Molecular Devices, USA) at 532 nm.

2.10 Immunohistochemistry

For this assay, the harvested tumor tissues were fixed in 4% paraformaldehyde for 24 h, embedded in paraffin and cut into 5-μm sections. The tissue sections were incubated with the indicated antibodies after which the signals were detected using biotinylated secondary antibodies and color development with DAB (3,3′-diaminobenzidine).

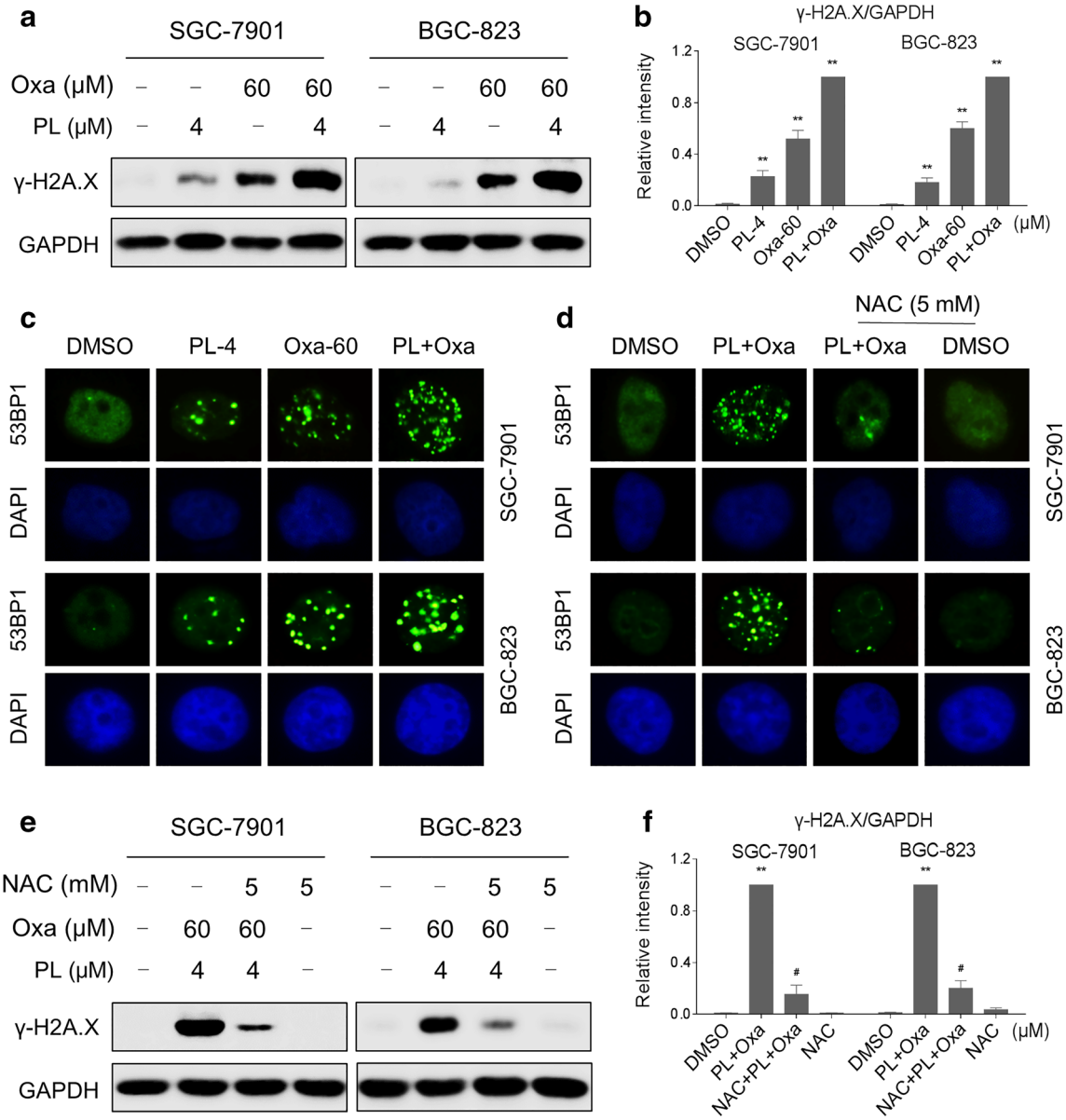

Fig. 3 PL and oxaliplatin combination treatment induces DNA damage in gastric cancer cells. ab SGC-7901 and BGC-823 cells were treated with PL or oxaliplatin alone or their combination at the indicated doses. At 20 h after treatment, the expression of γH2A.X was determined by Western blotting. GAPDH was used as internal control. **c** SGC-7901 and BGC-823 cells were treated with PL (4 μM) or oxaliplatin (60 μM) alone or their combination (4 μM PL and 60 μM oxaliplatin). At 20 h after treatment, nuclear foci formation of 53BPl was determined by immunofluorescence staining. **d** SGC-7901 and BGC-823 cells were pretreated with 5 mM NAC for 2 h before exposure to PL (4 μM) and oxaliplatin (60 μM) combination. At 20 h after treatment, nuclear foci formation of 53BPl was determined by immunofluorescence staining. **e-f** SGC-7901 and BGC-823 cells were pretreated with 5 mM NAC for 2 h before exposure to PL (4 μM) and oxaliplatin (60 μM) combination. At 20 h after treatment, the expression of γH2A.X was determined by Western blotting. GAPDH was used as internal control. Data represent similar results from three independent experiments (* $p < 0.05$, ** $p < 0.01$)

2.11 Statistical analysis

All experiments were performed in triplicate. The data are reported as means ± SEM. All statistical analyses were performed using GraphPad Prism 5.0. Student's t test and two-way ANOVA were employed to analyze the differences between data sets. A p value < 0.05 was considered statistically significant.

3 Results

3.1 PL synergistically increases the cytotoxicity of oxaliplatin in cancer cells

To determine whether PL can synergize with oxaliplatin to kill cancer cells, we first tested the effect of PL or oxaliplatin alone

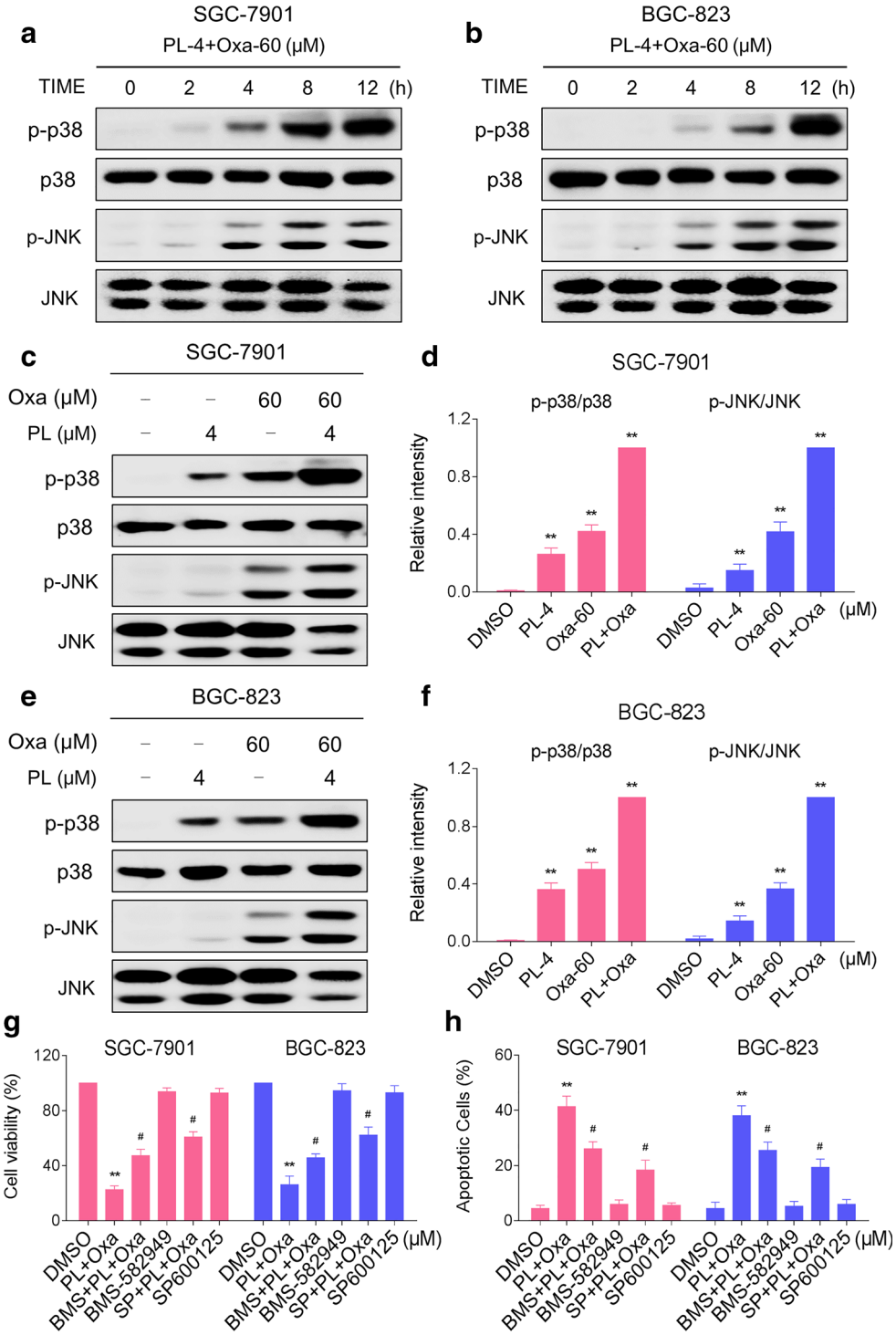

Fig. 4 PL and oxaliplatin combination activates p38 and JNK signaling pathways. a-b SGC-7901 and BGC-823 cells were treated with PL and oxaliplatin combination for the indicated time periods, after which the protein levels of p-p38, p38, p-JNK and JNK were determined by Western blotting. **c-f** SGC-7901 and BGC-823 cells were treated with PL or oxaliplatin alone or their combination at the indicated doses. At 12 h after treatment, the protein levels of p-p38, p38, p-JNK and JNK were determined by Western blotting. **g** SGC-7901 and BGC-823 cells were pretreated with BMS-582949 (10 μM) or SP600125 (20 μM) for 2 h before exposure to PL (4 μM) and oxaliplatin (60 μM) combination for 24 h, after which cell viability was determined by MTT assay. **h** SGC-7901 and BGC-823 cells were pretreated with BMS-582949 (10 μM) or SP600125 (20 μM) for 2 h before exposure to PL (4 μM) and oxaliplatin (60 μM) combination for 24 h, after which apoptosis was determined by flow cytometry. The percentage of apoptotic cells in the treatment groups was calculated. Data represent similar results from three independent experiments (* $p < 0.05$, ** $p < 0.01$)

or their combination on the viability of SGC-7901, BGC-823, AGS and HCT116 cells. Using a MTT assay, we found that 4 μM PL significantly increased the cytotoxicity of oxaliplatin in SGC-7901, BGC-823, AGS and HCT116 cells (Fig. 1a-b and Fig. S1A-S1B). The interaction of PL and oxaliplatin was calculated using combination index values (Fig. 1c-d and Fig, S1C-S1D) and showed that PL in combination with oxaliplatin exhibited a synergistic effect against both gastric and colon cancer cells. Furthermore, compared with PL or oxaliplatin treatment alone, we found that the combined treatment dramatically increased apoptosis in both SGC-7901 and BGC-823 cells (Fig. 1e-h). These results suggest that PL and oxaliplatin exhibit a synergistic effect against gastric and colon cancer cells.

3.2 PL and oxaliplatin cooperate to trigger ROS-dependent apoptosis

Next, we set out to investigate the mechanisms underlying the synergistic effect of PL and oxaliplatin. Previously, it has suggested that PL treatment may increase ROS levels in cancer cells, which may underlie its cancer cell-killing activity [19, 20]. Therefore, we measured the intracellular ROS levels after PL and oxaliplatin co-treatment. Time-course results indicated that the combined treatment significantly increased ROS levels in SGC-7901 and BGC-823 cells, and that these levels reached a peak at 2 h after treatment (Fig. 2a). In addition, we found that both the treatment with PL or oxaliplatin alone induced ROS generation, but that the combined treatment resulted in significantly increased ROS levels (Fig. 2b).

Intracellular ROS generation is known to play an important role in cancer cell apoptosis induced by various anticancer agents [26–28]. Therefore, we tested whether excessive ROS generation was involved in the synergistic effect of PL and oxaliplatin observed here. We found that pretreatment with NAC markedly reversed the combined treatment-induced increase in ROS levels (Fig. 2c). Using a MTT assay we additionally found that scavenging of ROS significantly attenuated the combined treatment-induced growth inhibition in both SGC-7901 and BGC-823 cells (Fig. 2d). These results were confirmed in HCT116 cells (Fig. S2A-S2B), and we also found that the combined treatment-induced apoptosis was blocked by NAC (Fig. 2e-h). These data suggest that ROS generation plays an essential role in the synergistic effect of PL and oxaliplatin.

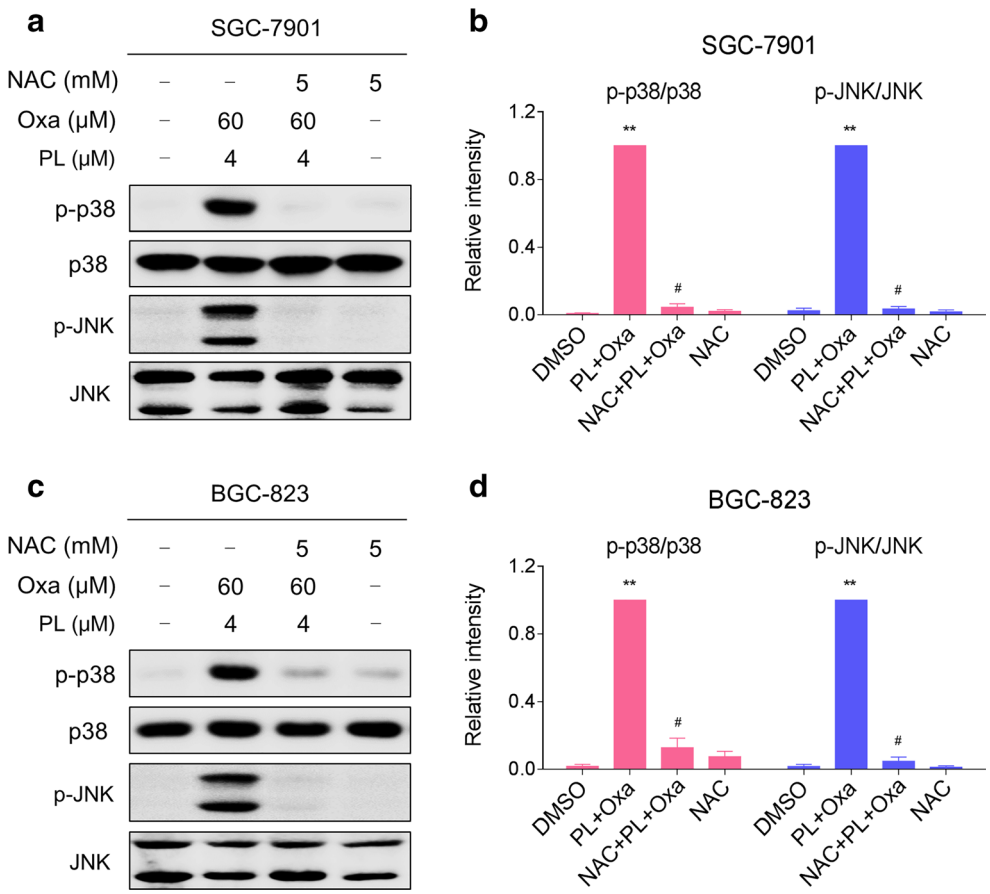

Fig. 5 Activation of the p38 and JNK signaling pathways is dependent on intracellular ROS generation. a-b SGC-7901 cells were pretreated with NAC (5 mM) for 2 h before exposure to PL (4 μM) and oxaliplatin (60 μM) combination. At 12 h after treatment, the protein levels of p-p38, p38, p-JNK and JNK were determined by Western blotting. **c-d** BGC-823 cells were pretreated with NAC (5 mM) for 2 h before exposure to PL (4 μM) and oxaliplatin (60 μM) combination. At 12 h after treatment, the protein levels of p-p38, p38, p-JNK and JNK were determined by Western blotting. Data represent similar results from three independent experiments (* $p < 0.05$, ** $p < 0.01$)

3.3 PL and oxaliplatin combination treatment induces DNA damage in gastric cancer cells

Excess ROS production has previously been shown to cause various cellular damages including DNA damage [29–31]. Therefore, we sought to investigate whether PL and oxaliplatin combination treatment can induce DNA damage in gastric cancer cells. Western blot analysis revealed that the combined treatment dramatically increased the level of γH2A.X in both SGC-7901 and BGC-823 cells (Fig. 3a-b). In addition, we found that the combined treatment resulted in an accumulation of nuclear 53BP1 foci, indicating an accumulation of double strand breaks in these cells (Fig. 3c). Next, we validated the interaction between ROS generation and DNA damage in gastric cancer cells. We found that inhibition of ROS production by NAC significantly attenuated the accumulation of nuclear 53BP1 foci and the expression of γH2A.X, indicating that DNA damage occurred downstream of ROS production (Fig. 3d-f).

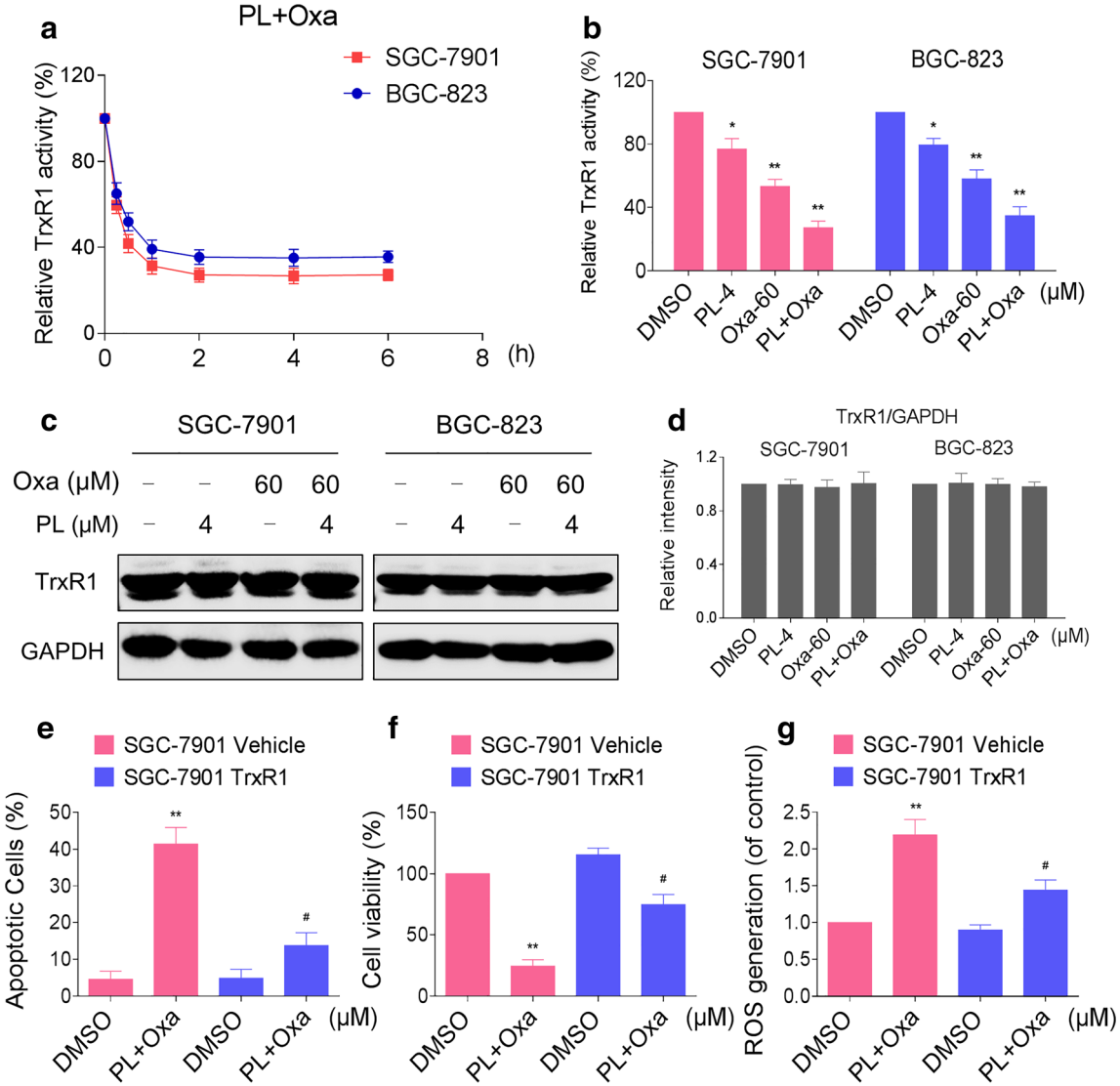

Fig. 6 PL and oxaliplatin combination inhibits TrxR1 activity in gastric cancer cells. a TrxR1 activity was measured in SGC-7901 and BGC-823 cells after treatment with the combination of PL (4 μM) and oxaliplatin (60 μM). **b** SGC-7901 and BGC-823 cells were treated with PL or oxaliplatin alone or their combination at the indicated doses. At 2 h after treatment xR1 activity was measured using an endpoint insulin reduction assay. **c-d** SGC-7901 and BGC-823 cells were treated with PL or oxaliplatin alone or their combination at the indicated doses. At 12 h after treatment the TrxR1 expression was determined by Western blotting. **e** SGC-7901-vehicle or SGC-7901-TrxR1 cells were treated with PL (4 μM) and oxaliplatin (60 μM) combination for 24 h, after which apoptosis was determined by flow cytometry. The percentage of apoptotic cells in the treatment groups was calculated. **f** SGC-7901-vehicle or SGC-7901-TrxR1 cells were treated with PL (4 μM) and oxaliplatin (60 μM) combination for 24 h, after which cell viability was determined by MTT assay. **g** SGC-7901-vehicle or SGC-7901-TrxR1 cells were treated with PL (4 μM) and oxaliplatin (60 μM) combination for 2 h, after which intracellular ROS levels were measured by flow cytometry. Data represent similar results from three independent experiments (* $p < 0.05$, ** $p < 0.01$)

3.4 PL and oxaliplatin combination activates ROS-mediated p38 and JNK signaling pathways

In response to ROS, the oxidized thioredoxin (Trx) form is released and subsequently activates ASK1 to mediate apoptosis via the p38 and JNK signaling pathways [32, 33]. Here, we hypothesize that activation of p38 and JNK signaling pathways contributes to gastric cancer cell apoptosis induced by the combined treatment. Time-course results indicated that the combined treatment indeed significantly activated the p38 and JNK signaling pathways in both SGC-7901 and BGC-823 cells (Fig. 4a-b). Furthermore, compared with PL or oxaliplatin treatment alone, we found that the combined treatment resulted in more significant increases in p38 and JNK phosphorylation levels in both SGC-7901 and BGC-823 cells (Fig. 4c-f). To further validate the involvement of the p38 and JNK signaling pathways in the synergistic effect of PL and oxaliplatin, SGC-7901 and BGC-823 cells were co-treated with PL and oxaliplatin after pretreatment with a p38 inhibitor (BMS-582949) or a JNK inhibitor (SP600125). We found that BMS-582949 or SP600125 partially attenuated combined treatment-induced growth inhibition and apoptosis in both SGC-7901 and BGC-823 cells (Fig. 4g-h). Moreover, we found that pretreatment with SP600125 and BMS-582949 significantly attenuated combined treatment-induced cell death in both SGC-7901 and BGC-823 cells, suggesting that activation of the p38 and JNK signaling pathways is essential for the combined treatment effect (Fig. S3A-S3B).

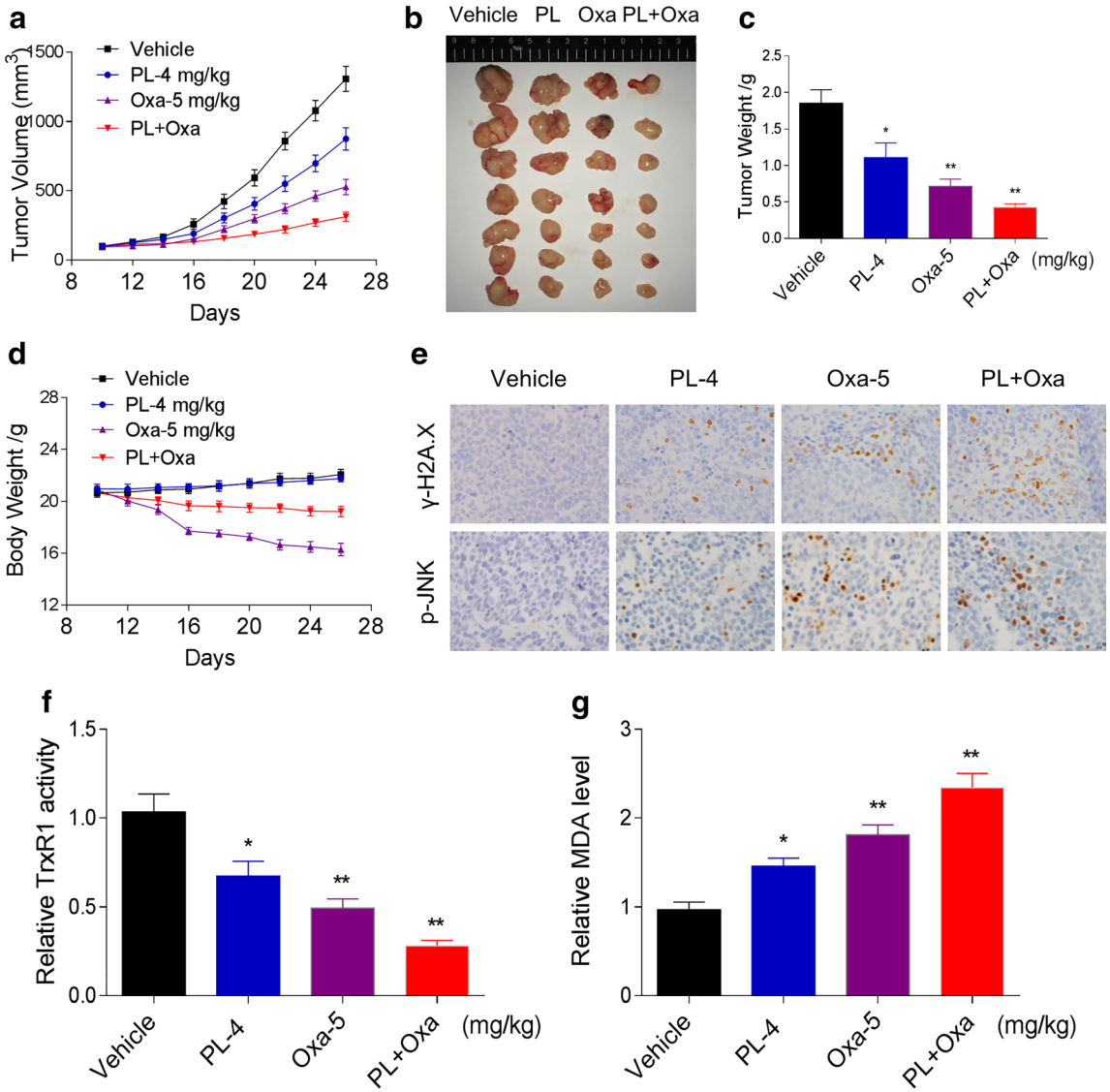

Fig. 7 PL and oxaliplatin combination inhibits SGC-7901 xenograft tumor growth in vivo, accompanied by decreased TrxR1 activity. a-b PL (4 mg/kg) and oxaliplatin (5 mg/kg) combined treatment significantly decreased tumor volume and tumor weight (**c**) of SGC-7901 human gastric cancer xenografts in nude mice. **d** Body weight of nude mice during the experiment. **e** Levels of γH2A.X and p-JNK in tumor tissues analyzed by immunohistochemistry. **f** Tumor tissues were lysed and proteins were used to determine TrxR1 activity using an endpoint insulin reduction assay. **g** MDA levels in the tumor tissues

We next tested the connection between ROS accumulation and activation of the p38 and JNK signaling pathways. We found that pretreatment with NAC markedly reversed the combined treatment-induced phosphorylation of p38 and JNK in both SGC-7901 and BGC-823 cells (Fig. 5a-d). We also were able to confirm these results in HCT116 cells (Fig. S4A-S4B). Taken together, these results suggest that activation of the p38 and JNK signaling pathways is due to accumulation of intracellular ROS in gastric cancer cells.

3.5 PL and oxaliplatin combination inhibits TrxR1 activity in gastric cancer cells

TrxR1 is an important regulator of the redox balance in cells and accumulating evidence indicates that intracellular ROS levels may be increased when TrxR1 activity is inhibited [24, 34, 35]. To test whether TrxR1 is involved in the synergistic effect observed, we measured TrxR1 activity after PL and oxaliplatin co-treatment. Using an endpoint insulin reduction assay to quantify inhibition of TrxR1 activity, we found that the PL and oxaliplatin combination significantly inhibited the TrxR1 activity in SGC-7901 and BGC-823 cells (Fig. 6a). Interestingly, we found that the TrxR1 activity was also inhibited by oxaliplatin and that the combined treatment exerted a stronger inhibitory effect on TrxR1 activity than either PL or oxaliplatin alone in both SGC-7901 and BGC-823 cells (Fig. 6b). Western blot analysis revealed that the expression level of TrxR1 did not significantly change after treatment with PL or oxaliplatin alone or their combination (Fig. 6c-d). To further validate the synergistic effect on TrxR1 activity inhibition, a TrxR1-overexpressing cell line (SGC-7901-TrxR1) was used. In doing so, we found that overexpression of TrxR1 markedly rescued the combined treatment-induced apoptosis, growth inhibition and ROS generation (Fig. 6e-g). These results indicate that the effects of PL and oxaliplatin to induce ROS and apoptosis are quantitatively linked to their ability to inhibit TrxR1 activity.

3.6 PL and oxaliplatin combination inhibits gastric tumor growth in vivo

To evaluate the in vivo effect of the combined treatment, we used a subcutaneous xenograft model of SGC-7901 cells in immunodeficient mice. After 17 days of treatment, we found that 4 mg/kg PL or 5 mg/kg oxaliplatin effectively inhibited the growth of SGC-7901 xenografts (Fig. 7a-c) and that the combined treatment exhibited a stronger inhibitory effect (Fig. 7a-c). Remarkably, we found that the administration of oxaliplatin (5 mg/kg) resulted in a significant weight loss, whereas the combined treatment was well-tolerated, suggesting that PL can attenuate the side effects of oxaliplatin (Fig. 7d). These results were confirmed using a subcutaneous xenograft model of HCT116 cells in immunodeficient mice (Fig. S5A-S5D). Mechanistically, we found by immunohistochemical staining that the expression of γ-H2A.X and p-JNK were significantly increased by the combined treatment (Fig. 7e). Moreover, we measured the TrxR1 activity in tumor tissues using an endpoint insulin reduction assay, and found that the combined treatment significantly decreased the activity of TrxR1 in the tumor tissues (Fig. 7f). In addition, we found that the combined treatment significantly increased the level of lipid peroxidation product (MDA), a marker of ROS, in the tumor tissues (Fig. 7g). Taken together, these results indicate that PL may synergize the effect of oxaliplatin to inhibit in vivo tumor growth by inhibiting TrxR1 activity, which is in accordance with the mechanism observed in vitro.

4 Discussion

The use of conventional chemotherapeutic drugs, including oxaliplatin, is limited due to toxicities and drug resistance. Recently, the combination of naturally occurring compounds with conventional chemotherapeutic drugs has gained attention [36, 37]. Here, we found that the combination of PL and oxaliplatin resulted in a marked increase in cell death in gastric cancer cells. This synergistic effect was found to occur primarily through inhibition of TrxR1 activity and increased generation of intracellular ROS, upstream events of DNA damage induction and p38 and JNK signaling pathway activation (Fig. 8). In vivo, we found that PL combined with oxaliplatin exhibited a synergistic inhibitory effect on gastric tumor growth, and effectively reduced the activity of TrxR1 in tumor tissues, which was consistent with the in vitro results.

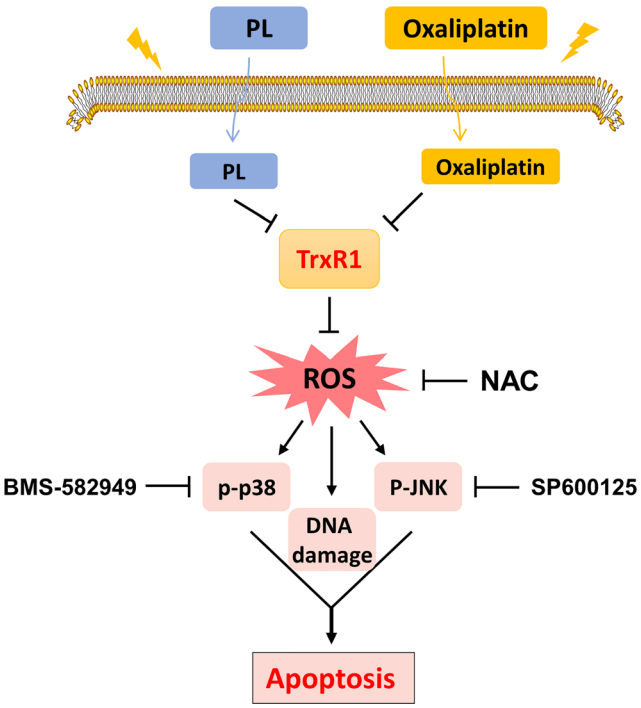

Fig. 8 Schematic illustration of the main findings of the present study

Remarkably, we found that PL attenuated the body weight loss evoked by oxaliplatin treatment, indicating that the effect of PL is cell-type dependent [38]. Elucidation of the underlying mechanisms warrants further study.

Cancer cells usually generate and maintain higher ROS levels compared to normal cells. Elevated ROS levels render cancer cells more sensitive to agents that increase ROS generation [39, 40]. Therefore, stimulation of ROS is a potential therapeutic strategy for cancer treatment. Numerous studies have shown that elevation of ROS production in cancer cells may lead to growth inhibition and apoptosis [29, 41]. Here, we found that combined PL and oxaliplatin treatment resulted in significant increases in ROS levels, and that pretreatment with NAC fully reversed this combined treatment-induced effect, suggesting that ROS play a critical role in the synergistic effect of PL and oxaliplatin. In addition, oxaliplatin is known to exert its cytotoxicity in cancer cells by inducing DNA damage [42]. Here, we found that PL enhanced DNA damage induced by oxaliplatin based on increases in nuclear 53BP1 foci and γH2A.X expression levels. Moreover, we found that pretreatment with NAC significantly attenuated the accumulation of nuclear 53BP1 foci and γH2A.X expression levels, indicating that DNA damage occurred downstream of ROS production. These results suggest that PL may serve as a novel agent to augment ROS production and to sensitize cancer cells to chemotherapeutic drugs.

By inducing ROS generation and oxidative stress, we found that the combined PL and oxaliplatin treatment concomitantly activated the p38 and JNK signaling pathways, as indicated by increased phosphorylation of both p38 and JNK. Moreover, we found that BMS-582949 or SP600125 could partially attenuate the combined treatment-induced cell growth inhibition and apoptosis, suggesting that activation of the p38 and JNK signaling pathways is essential for the effect of the combined treatment. In addition, we found that pretreatment with NAC markedly reversed the combined treatment-induced phosphorylation of p38 and JNK, suggesting that activation of the p38 and JNK signaling pathways is due to accumulation of intracellular ROS.

Understanding the molecular mechanisms underlying the antitumor effect of oxaliplatin may optimize the design of oxaliplatin-based combination therapies, which may improve its efficacy and minimize its adverse effects. Accumulating evidence indicates that intracellular ROS levels may be increased by TrxR1 inhibition [34, 43]. Accordingly, we found that TrxR1 activity in gastric cancer cells was decreased after combined PL and oxaliplatin treatment. Interestingly, we found that the TrxR1 activity was also significantly inhibited by oxaliplatin treatment, which is consistent with previous observations [44]. Moreover, we found that overexpression of TrxR1 significantly rescued the combined treatment-induced ROS generation, cell growth inhibition and apoptosis, suggesting that the synergistic effects of PL and oxaliplatin are quantitatively linked to their ability to inhibit TrxR1 activity. However, overexpression of TrxR1 did not completely rescue the combined treatment effects, indicating that other proteins such as GSTP1 and CBR1 may be involved in the synergistic effect of PL and oxaliplatin [21, 45].

In conclusion, we found that PL enhanced the antitumor effect of oxaliplatin by inhibiting TrxR1 activity, and showed that the combined treatment induced apoptotic cell death through ROS-mediated DNA damage and activation of the p38 and JNK signaling pathways. These findings provide new insights into the molecular mechanisms by which PL synergizes with oxaliplatin, and suggest that such a combinatorial treatment may become a more effective way to treat gastric cancer. Administration of PL as a chemosensitizer to oxaliplatin in gastric cancer warrants further consideration and clinical evaluation.

Author contributions Peng Zou and Yiqun Xia designed the study, supervised the project and wrote the manuscript. Peichen Zhang, Lingyan Shi and Tingting Zhang designed and performed most of the experiments. Lin Hong carried out the immunofluorescence experiments. Wei He, Peihai Cao, Xin Shen and Peisen Zheng collected and analyzed the data. All authors were involved in the final version of the manuscript.

Funding This research was supported by the National Natural Science Foundation of China (81603153 and 81503107) and the Zhejiang Provincial Natural Science Foundation of China (LY16H310011).

Data availability All data generated or analyzed during the present study are included in this publication.

Compliance with ethical standards

Competing interests The authors declare that they have no competing interests.

Ethics approval and consent to participate The experimental protocol was established according to the Guide for the Care and Use of Laboratory Animals, and was approved by the Institutional Animal Care and Use Committee of Wenzhou Medical University.

References

1. K. Shitara, K. Chin, T. Yoshikawa, H. Katai, M. Terashima, S. Ito, M. Hirao, K. Yoshida, E. Oki, M. Sasako, Y. Emi, T. Tsujinaka, Phase II study of adjuvant chemotherapy of S-1 plus oxaliplatin for patients with stage III gastric cancer after D2 gastrectomy. Gastric Cancer **20**, 175–181 (2017). https://doi.org/10.1007/s10120-015-0581-1
2. S.H. Noh, S.R. Park, H.K. Yang, H.C. Chung, I.J. Chung, S.W. Kim, H.H. Kim, J.H. Choi, H.K. Kim, W. Yu, J.I. Lee, D.B. Shin, J. Ji, J.S. Chen, Y. Lim, S. Ha, Y.J. Bang, Adjuvant capecitabine plus oxaliplatin for gastric cancer after D2 gastrectomy (CLASSIC): 5-year follow-up of an open-label, randomised phase 3 trial. Lancet Oncol. **15**, 1389–1396 (2014). https://doi.org/10.1016/S1470-2045(14)70473-5
3. E. Van Cutsem, X. Sagaert, B. Topal, K. Haustermans, H. Prenen, Gastric cancer. Lancet **388**, 2654–2664 (2016). https://doi.org/10.1016/S0140-6736(16)30354-3

4. E.C. Smyth, M. Verheij, W. Allum, D. Cunningham, A. Cervantes, D. Arnold, Gastric cancer: ESMO clinical practice guidelines for diagnosis, treatment and follow-up. Ann. Oncol. **27**, v38–v49 (2016). https://doi.org/10.1093/annonc/mdw350
5. Y.J. Bang, Y.W. Kim, H.K. Yang, H.C. Chung, Y.K. Park, K.H. Lee, K.W. Lee, Y.H. Kim, S.I. Noh, J.Y. Cho, Y.J. Mok, J. Ji, T.S. Yeh, P. Button, F. Sirzen, S.H. Noh, Adjuvant capecitabine and oxaliplatin for gastric cancer after D2 gastrectomy (CLASSIC): A phase 3 open-label, randomised controlled trial. Lancet **379**, 315–321 (2012). https://doi.org/10.1016/S0140-6736(11)61873-4
6. E. Gamelin, L. Gamelin, L. Bossi, S. Quasthoff, Clinical aspects and molecular basis of oxaliplatin neurotoxicity: Current management and development of preventive measures. Sem. Oncol. **29**, 21–33 (2002). https://doi.org/10.1053/sonc.2002.35525
7. M. Cebula, E.E. Schmidt, E.S. Arner, TrxR1 as a potent regulator of the Nrf2-Keap1 response system. Antioxid. Redox Signal. **23**, 823–853 (2015). https://doi.org/10.1089/ars.2015.6378
8. H. Esen, F. Erdi, B. Kaya, B. Feyzioglu, F. Keskin, L.S. Demir, Tissue thioredoxin reductase-1 expression in astrocytomas of different grades. J. Neuro-Oncol. **121**, 451–458 (2015). https://doi.org/10.1007/s11060-014-1661-5
9. W. Zhang, X. Zheng, X. Wang, Oxidative stress measured by thioredoxin reductase level as potential biomarker for prostate cancer. Am. J. Cancer Res. **5**, 2788–2798 (2015)
10. W.C. Stafford, X. Peng, M.H. Olofsson, X. Zhang, D.K. Luci, L. Lu, Q. Cheng, L. Tresaugues, T.S. Dexheimer, N.P. Coussens, M. Augsten, H.M. Ahlzen, O. Orwar, A. Ostman, S. Stone-Elander, D.J. Maloney, A. Jadhav, A. Simeonov, S. Linder and E.S.J. Arner, Irreversible inhibition of cytosolic thioredoxin reductase 1 as a mechanistic basis for anticancer therapy. Science Transl. Med. **10**, (2018) https://doi.org/10.1126/scitranslmed.aaf7444
11. X. Zheng, W. Ma, R. Sun, H. Yin, F. Lin, Y. Liu, W. Xu, H. Zeng, Butaselen prevents hepatocarcinogenesis and progression through inhibiting thioredoxin reductase activity. Redox Biol. **14**, 237–249 (2018). https://doi.org/10.1016/j.redox.2017.09.014
12. P.V. Raninga, G. Di Trapani, S. Vuckovic, K.F. Tonissen, TrxR1 inhibition overcomes both hypoxia-induced and acquired bortezomib resistance in multiple myeloma through NF-small ka, cyrillicbeta inhibition. Cell Cycle **15**, 559–572 (2016). https://doi.org/10.1080/15384101.2015.1136038
13. C. Fan, W. Zheng, X. Fu, X. Li, Y.S. Wong, T. Chen, Enhancement of auranofin-induced lung cancer cell apoptosis by selenocystine, a natural inhibitor of TrxR1 in vitro and in vivo. Cell Death Dis **5**, e1191 (2014). https://doi.org/10.1038/cddis.2014.132
14. W. Cai, L. Zhang, Y. Song, B. Wang, B. Zhang, X. Cui, G. Hu, Y. Liu, J. Wu, J. Fang, Small molecule inhibitors of mammalian thioredoxin reductase. Free Rad. Biol. Med. **52**, 257–265 (2012). https://doi.org/10.1016/j.freeradbiomed.2011.10.447
15. W. Fiskus, N. Saba, M. Shen, M. Ghias, J. Liu, S.D. Gupta, L. Chauhan, R. Rao, S. Gunewardena, K. Schorno, C.P. Austin, K. Maddocks, J. Byrd, A. Melnick, P. Huang, A. Wiestner, K.N. Bhalla, Auranofin induces lethal oxidative and endoplasmic reticulum stress and exerts potent preclinical activity against chronic lymphocytic leukemia. Cancer Res. **74**, 2520–2532 (2014). https://doi.org/10.1158/0008-5472.CAN-13-2033
16. Y. Liu, D. Duan, J. Yao, B. Zhang, S. Peng, H. Ma, Y. Song, J. Fang, Dithiaarsanes induce oxidative stress-mediated apoptosis in HL-60 cells by selectively targeting thioredoxin reductase. J. Med. Chem. **57**, 5203–5211 (2014). https://doi.org/10.1021/jm500221p
17. W. Hang, Z.X. Yin, G. Liu, Q. Zeng, X.F. Shen, Q.H. Sun, D.D. Li, Y.P. Jian, Y.H. Zhang, Y.S. Wang, C.S. Quan, R.X. Zhao, Y.L. Li, Z.X. Xu, Piperlongumine and p53-reactivator APR-246 selectively induce cell death in HNSCC by targeting GSTP1. Oncogene **37**, 3384–3398 (2018). https://doi.org/10.1038/s41388-017-0110-2
18. T.H. Kim, J. Song, S.H. Kim, A.K. Parikh, X. Mo, K. Palanichamy, B. Kaur, J. Yu, S.O. Yoon, I. Nakano, C.H. Kwon, Piperlongumine treatment inactivates peroxiredoxin 4, exacerbates endoplasmic reticulum stress, and preferentially kills high-grade glioma cells. Neuro-Oncol. **16**, 1354–1364 (2014). https://doi.org/10.1093/neuonc/nou088
19. S. Thongsom, W. Suginta, K.J. Lee, H. Choe, C. Talabnin, Piperlongumine induces G2/M phase arrest and apoptosis in cholangiocarcinoma cells through the ROS-JNK-ERK signaling pathway. Apoptosis **22**, 1473–1484 (2017). https://doi.org/10.1007/s10495-017-1422-y
20. K. Karki, E. Hedrick, R. Kasiappan, U.H. Jin, S. Safe, Piperlongumine induces reactive oxygen species (ROS)-dependent downregulation of specificity protein transcription factors. Cancer Prev. Res. **10**, 467–477 (2017). https://doi.org/10.1158/1940-6207.CAPR-17-0053
21. H. Wang, H. Jiang, C. Corbet, S. de Mey, K. Law, T. Gevaert, O. Feron, M. De Ridder, Piperlongumine increases sensitivity of colorectal cancer cells to radiation: Involvement of ROS production via dual inhibition of glutathione and thioredoxin systems. Cancer Lett. **450**, 42–52 (2019). https://doi.org/10.1016/j.canlet.2019.02.034
22. D. Chen, Y. Ma, P. Li, M. Liu, Y. Fang, J. Zhang, B. Zhang, Y. Hui and Y. Yin, Piperlongumine induces apoptosis and synergizes with doxorubicin by inhibiting the JAK2-STAT3 pathway in triple-negative breast cancer. Molecules **24**, (2019) https://doi.org/10.3390/molecules24122338
23. J. Mohammad, H. Dhillon, S. Chikara, S. Mamidi, A. Sreedasyam, K. Chittem, M. Orr, J.C. Wilkinson, K.M. Reindl, Piperlongumine potentiates the effects of gemcitabine in in vitro and in vivo human pancreatic cancer models. Oncotarget **9**, 10457–10469 (2018). https://doi.org/10.18632/oncotarget.23623
24. P. Zou, Y. Xia, J. Ji, W. Chen, J. Zhang, X. Chen, V. Rajamanickam, G. Chen, Z. Wang, L. Chen, Y. Wang, S. Yang, G. Liang, Piperlongumine as a direct TrxR1 inhibitor with suppressive activity against gastric cancer. Cancer Lett. **375**, 114–126 (2016). https://doi.org/10.1016/j.canlet.2016.02.058
25. T.C. Chou, Drug combination studies and their synergy quantification using the Chou-Talalay method. Cancer Res. **70**, 440–446 (2010). https://doi.org/10.1158/0008-5472.CAN-09-1947
26. S.L. Locatelli, L. Cleris, G.G. Stirparo, S. Tartari, E. Saba, M. Pierdominici, W. Malorni, A. Carbone, A. Anichini, C. Carlo-Stella, BIM upregulation and ROS-dependent necroptosis mediate the antitumor effects of the HDACi Givinostat and Sorafenib in Hodgkin lymphoma cell line xenografts. Leukemia **28**, 1861–1871 (2014). https://doi.org/10.1038/leu.2014.81
27. X. Wang, Q. Guo, L. Tao, L. Zhao, Y. Chen, T. An, Z. Chen, R. Fu, E platinum, a newly synthesized platinum compound, induces apoptosis through ROS-triggered ER stress in gastric carcinoma cells. Mol. Carc. **56**, 218–231 (2017). https://doi.org/10.1002/mc.22486
28. Z.H. Tang, W.X. Cao, M.X. Su, X. Chen, J.J. Lu, Osimertinib induces autophagy and apoptosis via reactive oxygen species generation in non-small cell lung cancer cells. Toxicol. Appl. Pharmacol. **321**, 18–26 (2017). https://doi.org/10.1016/j.taap.2017.02.017
29. N. Liu, K.S. Wang, M. Qi, Y.J. Zhou, G.Y. Zeng, J. Tao, J.D. Zhou, J.L. Zhang, X. Chen, C. Peng, Vitexin compound 1, a novel extraction from a Chinese herb, suppresses melanoma cell growth through DNA damage by increasing ROS levels. J. Exp. Clin. Cancer Res. **37**, 269 (2018). https://doi.org/10.1186/s13046-018-0897-x
30. M. Schieber, N.S. Chandel, ROS function in redox signaling and oxidative stress. Curr. Biol. **24**, R453–R462 (2014). https://doi.org/10.1016/j.cub.2014.03.034
31. A. Zafar, S. Singh, I. Naseem, Cu(II)-coumestrol interaction leads to ROS-mediated DNA damage and cell death: A putative mechanism for anticancer activity. J. Nutrit. Biochem. **33**, 15–27 (2016). https://doi.org/10.1016/j.jnutbio.2016.03.003
32. C.C. Hsieh, J. Papaconstantinou, Thioredoxin-ASK1 complex levels regulate ROS-mediated p38 MAPK pathway activity in

livers of aged and long-lived Snell dwarf mice. FASEB J. **20**, 259–268 (2006). https://doi.org/10.1096/fj.05-4376com
33. M.D. Mantzaris, S. Bellou, V. Skiada, N. Kitsati, T. Fotsis, D. Galaris, Intracellular labile iron determines H2O2-induced apoptotic signaling via sustained activation of ASK1/JNK-p38 axis. Free Radic. Biol. Med. **97**, 454–465 (2016). https://doi.org/10.1016/j.freeradbiomed.2016.07.002
34. D. Duan, J. Zhang, J. Yao, Y. Liu, J. Fang, Targeting thioredoxin reductase by parthenolide contributes to inducing apoptosis of HeLa cells. J. Biol. Chem. **291**, 10021–10031 (2016). https://doi.org/10.1074/jbc.M115.700591
35. D. Duan, B. Zhang, J. Yao, Y. Liu, J. Fang, Shikonin targets cytosolic thioredoxin reductase to induce ROS-mediated apoptosis in human promyelocytic leukemia HL-60 cells. Free Radic. Biol. Med. **70**, 182–193 (2014). https://doi.org/10.1016/j.freeradbiomed.2014.02.016
36. H.M. Abdallah, A.M. Al-Abd, R.S. El-Dine, A.M. El-Halawany, P-glycoprotein inhibitors of natural origin as potential tumor chemosensitizers: A review. J. Adv. Res. **6**, 45–62 (2015). https://doi.org/10.1016/j.jare.2014.11.008
37. A. Bishayee, G. Sethi, Bioactive natural products in cancer prevention and therapy: Progress and promise. Sem. Cancer Biol. **40-41**, 1–3 (2016). https://doi.org/10.1016/j.semcancer.2016.08.006
38. S. Peng, B. Zhang, X. Meng, J. Yao, J. Fang, Synthesis of piperlongumine analogues and discovery of nuclear factor erythroid 2-related factor 2 (Nrf2) activators as potential neuroprotective agents. J. Med. Chem. **58**, 5242–5255 (2015). https://doi.org/10.1021/acs.jmedchem.5b00410
39. D. Trachootham, J. Alexandre, P. Huang, Targeting cancer cells by ROS-mediated mechanisms: A radical therapeutic approach? Nature Rev. Drug Discov. **8**, 579–591 (2009). https://doi.org/10.1038/nrd2803
40. C. Gorrini, I.S. Harris, T.W. Mak, Modulation of oxidative stress as an anticancer strategy. Nature Rev. Drug Discov. **12**, 931–947 (2013). https://doi.org/10.1038/nrd4002
41. Y. Yang, Y. Zhang, L. Wang, S. Lee, Levistolide A induces apoptosis via ROS-mediated ER stress pathway in colon cancer cells. Cell. Physiol. Biochem. **42**, 929–938 (2017). https://doi.org/10.1159/000478647
42. Y. Jung, S.J. Lippard, Direct cellular responses to platinum-induced DNA damage. Chem. Rev. **107**, 1387–1407 (2007). https://doi.org/10.1021/cr068207j
43. K. Li, Q. Zheng, X. Chen, Y. Wang, D. Wang, J. Wang, Isobavachalcone induces ROS-mediated apoptosis via targeting thioredoxin reductase 1 in human prostate cancer PC-3 cells. Oxid. Med. Cell. Longevity **2018**, 1915828–1915813 (2018). https://doi.org/10.1155/2018/1915828
44. A.B. Witte, K. Anestal, E. Jerremalm, H. Ehrsson, E.S. Arner, Inhibition of thioredoxin reductase but not of glutathione reductase by the major classes of alkylating and platinum-containing anticancer compounds. Free Radic. Biol. Med. **39**, 696–703 (2005). https://doi.org/10.1016/j.freeradbiomed.2005.04.025
45. K. Piska, P. Koczurkiewicz, D. Wnuk, E. Karnas, A. Bucki, K. Wojcik-Pszczola, M. Jamrozik, M. Michalik, M. Kolaczkowski, E. Pekala, Synergistic anticancer activity of doxorubicin and piperlongumine on DU-145 prostate cancer cells - the involvement of carbonyl reductase 1 inhibition. Chem. Biol. Interact. **300**, 40–48 (2019). https://doi.org/10.1016/j.cbi.2019.01.003

Affiliations

Peichen Zhang [1] · Lingyan Shi [2] · Tingting Zhang [3] · Lin Hong [3] · Wei He [3] · Peihai Cao [3] · Xin Shen [3] · Peisen Zheng [3] · Yiqun Xia [2] · Peng Zou [3]

[1] Department of Gastrointestinal Surgery, The First Affiliated Hospital of Wenzhou Medical University, Wenzhou Medical University, Wenzhou, Zhejiang 325035, China

[2] Department of Gastroenterology and Hepatology, The First Affiliated Hospital of Wenzhou Medical University, Wenzhou Medical University, Wenzhou, Zhejiang 325035, China

[3] Chemical Biology Research Center, School of Pharmaceutical Sciences, Wenzhou Medical University, Wenzhou, Zhejiang 325035, China